Vol. 376: 69–83, 2009
doi: 10.3354/meps07748

MARINE ECOLOGY PROGRESS SERIES
Mar Ecol Prog Ser

Published February 11

Chain model of phytoplankton P, N and light colimitation

Markus Pahlow*, Andreas Oschlies

IFM-GEOMAR, Düsternbrooker Weg 20, 24105 Kiel, Germany

ABSTRACT: Models of multiple potentially limiting nutrients currently employ either multiplicative or threshold formulations, neither of which has a sound mechanistic explanation. Despite experimental evidence that lack of P severely constrains N assimilation, this mechanism has not been considered for constructing models of multi-nutrient limitation. We construct a phytoplankton optimal growth model linking C, chlorophyll (Chl), N, and P through a limitation chain in which P limits N assimilation, N limits photosynthesis and photosynthesis limits growth. The resulting formulation possesses characteristics of both multiplicative and threshold approaches and provides a mechanistic foundation for modelling multi-nutrient and light limitation of phytoplankton growth. The model compares well with experimental observations for a variety of unicellular phytoplankton species. It is suggested that the widely held view that N and P limitation act independently of each other is based on an invalid interpretation of experimental observations and that the transition from N to P limitation occurs over a wide range of colimitation rather than a sharply-defined transition point. If the species considered in this study are representative for marine phytoplankton, our model results indicate that most phytoplankton are colimited by N and P when inorganic N and P are simultaneously exhausted in the surface ocean. The model suggests that the close match between marine inorganic (Redfield) and phytoplankton N:P ratios results from optimal nutrient utilisation but does not indicate optimality of Redfield N:P.

KEY WORDS: N · P · Light colimitation · Redfield C:N:P · Chlorophyll dynamics

INTRODUCTION

The cell quota model was developed to describe the relationship between elemental composition and C-based growth rate (μ) in phytoplankton (Droop 1973). For any potentially limiting nutrient n, the effect of its cell quota Q^n on phytoplankton growth rate is described by

$$f^n = 1 - \frac{Q_0^n}{Q^n} \quad (1)$$

where the cell quota Q^n is the ratio of n to biomass (C), and Q_0^n is the subsistence or minimum quota. The cell-quota approach has been used to construct phytoplankton growth models describing the interactions of light and nutrient limitation (e.g. Laws & Chalup 1990, Geider et al. 1998), but few attempts have been made to include effects of different nutrient elements in a mechanistic theory (Flynn 2001, Flynn 2008). Colimitation by several nutrients has been classified on a theoretical basis by Arrigo (2005), who distinguished direct effects of nutrient concentration (multi-nutrient colimitation), organism-level effects (biochemical colimitation) and population-level effects (community colimitation). More recently, Saito et al. (2008) further distinguished organism-level effects as independent, biochemical substitution and biochemically dependent colimitation. The most common treatment of the effects several potentially limiting nutrients may have on phytoplankton growth uses either multiplicative or threshold formulae to combine the respective individual effects (e.g. Terry 1980):

$$\mu = \mu_{max} \cdot f^{n_1} \cdot f^{n_2} \ldots \quad \text{or} \quad \mu = \mu_{max} \cdot \min(f^{n_1}, f^{n_2}, \ldots) \quad (2)$$

*Email: mpahlow@ifm-geomar.de

which fall into the category of independent nutrient colimitation *sensu* Saito et al. (2008), as the limitation term f^{n1} for nutrient n_1 is independent of nutrient n_2 and vice versa. Colimitation is the simultaneous limitation (reduction) of growth by several resources and can be contrasted with luxury uptake, where variation of the stoichiometry of non-limiting elements does not affect growth rates. In this respect, only the multiplicative form of Eq. (2) always describes colimitation, whereas the threshold function produces colimitation only if all f^n are equal. For simplicity, however, we will use the term colimitation model here to refer to the description of growth as a function of 2 or more potentially limiting nutrients that may or may not influence growth rates under a specific set of circumstances.

Because it is difficult to establish simultaneous limitation by several nutrients experimentally, the effects of several potentially limiting nutrients are usually examined by varying the concentration of one nutrient (assumed to be limiting) while keeping the others constant (assumed to be non-limiting). In such experiments, Q^P (P:C ratio) is more variable and behaves qualitatively different under P limitation than Q^N (N:C ratio) does under N limitation (e.g. Terry et al. 1985). A much more striking asymmetry is observed, however, for the non-limiting cell quota, i.e. between Q^P under N limitation and Q^N under P limitation (non-limiting cell quota): Q^P is much higher under N than under P limiting conditions for any given growth rate (Healey 1985, Terry et al. 1985), whereas the relationship between Q^N and growth rate is usually very similar for both N and P limitation (Laws & Bannister 1980, Terry 1980).

Formulations of independent colimitation are necessarily symmetrical with respect to different nutrient element cell quotas and thus cannot explain the asymmetrical behaviour of the non-limiting cell quota under N or P limitation. This is not to say that the experiments by Healey (1985) and Terry et al. (1985) are examples of N and P colimitation; however, regardless whether colimitation actually occurred, a colimitation model should be able to reproduce the differential behaviour of the limiting and non-limiting nutrient quotas in these experiments, while symmetrical models could not: the multiplicative formulation in Eq. (2) would necessarily require a higher cell quota of the non-limiting nutrient in both cases in order to achieve the same growth rate under otherwise identical conditions. The threshold formulation in Eq. (2) could principally be formulated in such a way that an asymmetric response is achieved, e.g. by imposing $f^N \leq f^P$, but this is not mechanistically motivated and would restrict the N:P ratio to below the value for light-limited growth (where $f^N = f^P = 1$) or below, which is usually exceeded for P limited growth. Flynn (2001) proposed an intermediate formulation allowing for some interaction between the effects of N and P limitation, but because the interaction term is symmetrical, it cannot explain the asymmetric behaviour of non-limiting N and P quotas (Fig. 6 in Flynn 2001). In order to achieve an asymmetric behaviour, Flynn (2008) pragmatically applied different multipliers *ad hoc* to non-limiting N and P transport.

Terry et al. (1985) interpreted the finding of an almost unique relationship between growth rate and Q^N over a wide range of supply N:P ratios as indicating that P limitation restricts N assimilation. This interpretation has not been used in phytoplankton growth models of multiple limiting nutrients, possibly due to a lack of evidence for interactions between effects of N and P limitation (Rhee 1978, Saito et al. 2008). Studies designed to detect colimitation, e.g. that of Rhee (1978), however, have focused exclusively on the difference between multiplicative and threshold formulations and have only considered independent colimitation. If N assimilation is controlled by P, N and P colimitation would instead have to be considered as biochemically dependent in terms of the classification proposed by Saito et al. (2008). P and N could be envisaged as a chain of limitations in which Q^P limits N assimilation and Q^N determines rates of growth and other processes (chain model, Ågren 2004). This concept is used here to extend a slightly simplified version of the optimal growth model of Pahlow (2005) to include P.

MODEL

Phytoplankton growth is usually described in terms of benefits only, e.g. as monotonically increasing functions of nutrient concentration or cell quota. Describing optimal growth requires the identification of trade-offs in terms of benefits and costs involved in chlorophyll (Chl) synthesis and nutrient assimilation. Two different kinds of costs can be distinguished, actual losses and allocation costs. Respiration covering the cost of biosynthesis is an example of an actual loss. Allocation costs are the result of competing requirements by different processes for limited cellular resources. For example, a larger allocation of N in the form of enzymes used for pigment synthesis will necessarily reduce its allocation for nutrient uptake. Optimality-based phytoplankton models have mostly focused on allocation (Shuter 1979, Armstrong 1999, Klausmeier et al. 2004a, Armstrong 2006), but Pahlow (2005) also considered the energetic cost of biosynthesis, and this is also done in the model presented here.

The model describes phytoplankton growth in terms of the dynamics of 4 state variables, C, N, P and Chl, representing the total biomass and composition of phytoplankton cells:

$$\frac{1}{C}\frac{dC}{dt} = \mu = \mu_g - R, \quad R = \zeta V^N + R_M \tag{3}$$

$$\frac{1}{N}\frac{dN}{dt} = \frac{V^N}{Q^N} - R_M \tag{4}$$

$$\frac{1}{P}\frac{dP}{dt} = \frac{V^P}{Q^P} - R_M \tag{5}$$

$$\frac{1}{Chl}\frac{dChl}{dt} = \mu^{Chl} = \frac{1}{\theta^C}\frac{d\theta^C}{dt} + \mu \tag{6}$$

where t is time, V^N and V^P are N and P assimilation rates per unit biomass, Q^N, Q^P and θ^C are cellular N:C, P:C and Chl:C ratios, R_M is maintenance respiration, and ζV^N defines the cost of biosynthesis proportional to N assimilation (Laws & Wong 1978, Geider et al. 1998). The cost of biosynthesis nevertheless is supposed to include all costs associated with active growth, including P assimilation, pigment synthesis, etc. The application of loss terms equal to R_M to N, P and Chl in Eqs. (3) to (6) is meant to represent losses due to, for example, leakage and decay of pigments (the same loss rate is applied to all compartments for mathematical convenience). All model variables and parameters are defined in Table 1. Expressions for μ_g, V^N, V^P, and $1/\theta^C \cdot d\theta^C/dt$ are derived by dividing the phytoplankton cell into idealised functional compartments (Fig. 1) and are based on the following set of assumptions.

(1) Regulation of nutrient uptake and Chl synthesis maximises balanced growth rate of the cell. Balanced growth means growth with constant cellular composition, i.e.

$$\frac{1}{C}\frac{dC}{dt} = \frac{1}{N}\frac{dN}{dt} = \frac{1}{P}\frac{dP}{dt} = \frac{1}{Chl}\frac{dChl}{dt} \tag{7}$$

(2) A constant amount of P per unit biomass (Q_0^P) is associated with DNA in the nucleus and phospholipids in membranes, both of which are expected to occur in relatively constant and similar proportions to biomass (Sterner & Elser 2002), and the remainder comprises ribosomes and RNA, responsible for protein biosynthesis (biosynthetic apparatus).

(3) A constant amount of N per unit biomass (Q_0^N) is used for the protoplast, with the remainder in the chloroplast.

(4) Assimilated N contributes to enzyme activity, because it is contained either directly in enzymes or in structural compounds necessary for enzyme activity.

(5) N assimilation can be split into 2 steps, uptake into the cell and assimilation into protein, whereby uptake is due to proteins of the uptake apparatus, assumed to form a constant fraction of Q_0^N (Fig. 1), and protein biosynthesis occurs at the ribosomes ($Q^P - Q_0^P$).

(6) The N:C ratio is the same in protoplast and chloroplast and the P:C ratio is the same everywhere within the protoplast, i.e. the P:C ratio of the biosynthetic apparatus equals protoplast P:C ratio.

(7) Biomass (C) is allocated to each compartment in proportion to its potential activity (energy (C) or nitrogen processing capacities of N and P associated compartments, respectively).

Table 1. Model variables and parameters

Variable	Units	Description
A	m^3 (mol C d)$^{-1}$	Affinity for inorganic nutrients
A_0	m^3 (mol N d)$^{-1}$	Affinity parameter
α	m^3 g C (µE g Chl)$^{-1}$	Light absorption coefficient
C	mmol m^{-3}	Phytoplankton C concentration[a]
Chl	mg m^{-3}	Phytoplankton Chl concentration
D	–	Daylength fraction
f_A	–	Fraction of Q_0 allocated for affinity
f_I^N	–	Relative N utilisation index
I	µE m^{-2} d^{-1}	Irradiance
μ	d^{-1}	Instantaneous growth rate
$\bar{\mu}$	d^{-1}	Average growth rate over 24 h
μ_*	d^{-1}	Daytime energy turnover capacity
μ_g	d^{-1}	Gross instantaneous growth rate
μ_{max}	d^{-1}	Maximal actual growth rate
n	–	Number of uptake sites
N	mmol m^{-3}	Phytoplankton N concentration
N_i	mmol m^{-3}	Inorganic N concentration
N_t	mmol m^{-3}	Inorganic N concentration in fresh medium
P	mmol m^{-3}	Phytoplankton P concentration
P_i	mmol m^{-3}	Inorganic P concentration
P_t	mmol m^{-3}	Inorganic P concentration in fresh medium
Q^N	mol N (mol C)$^{-1}$	Normalised N quota (N:C ratio)
Q_0^N	mol N (mol C)$^{-1}$	Subsistence N:C ratio
Q_{opt}^N	mol N (mol C)$^{-1}$	Optimal QN
Q^P	mol P (mol C)$^{-1}$	Normalised P quota (P:C ratio)
Q_0^P	mol P (mol C)$^{-1}$	Subsistence P:C ratio
Q_{max}^P	mol P (mol C)$^{-1}$	Maximal QP
R	d^{-1}	Respiration
R_M	d^{-1}	Maintenance respiration
S_I	–	Light saturation
θ^C	g Chl (g C)$^{-1}$	Chl:C ratio
$\hat{\theta}^C$	g Chl (g C)$^{-1}$	Chloroplast Chl:C ratio
V^N	mol N (mol C d)$^{-1}$	N assimilation rate
$\widetilde{V^N}$	mol N (mol C d)$^{-1}$	Unregulated N uptake rate
V_0^N	mol N (mol C d)$^{-1}$	N assimilation capacity of protoplast
V_{max}^N	mol N (mol C d)$^{-1}$	Maximum N uptake rate
V^P	mol P (mol C d)$^{-1}$	P assimilation rate
$\widetilde{V^P}$	mol P (mol C d)$^{-1}$	Unregulated P uptake rate
V_0^P	mol P (mol C d)$^{-1}$	P assimilation capacity of protoplast
V_{max}^P	mol P (mol C d)$^{-1}$	Maximum P uptake rate
ξ	g C (g Chl)$^{-1}$	C associated with Chl
ζ	mol C (mol N)$^{-1}$	Cost of biosynthesis coefficient

[a]Units are mg m^{-3} in combination with Chl

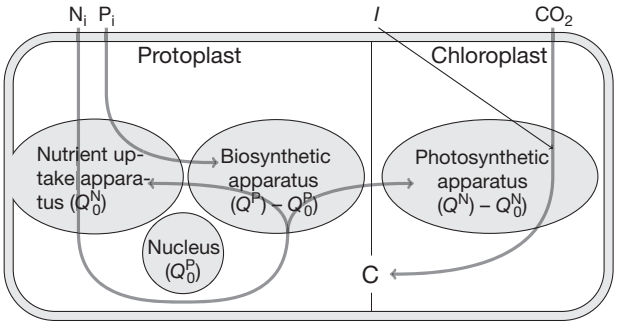

Fig. 1. Model compartments and associated partial nutrient quotas for N and P. The protoplast consists of the cell wall with the nutrient uptake apparatus (associated with partial N quota), the nucleus (Q_0^P) and the biosynthetic apparatus ($Q^P - Q_0^P$), and the chloroplast contains the photosynthetic apparatus ($Q^N - Q_0^N$)

Assumptions 1 to 4 define the idealised compartments and Assumption 5 stipulates that N assimilation depends on Q^P, which causes an asymmetry between effects of N and P because there is no corresponding effect of Q^N on P assimilation. Assumptions 6 and 7 define biomass (C) as a common frame of reference for modelling the effects of N and P.

The idealised compartments are defined with respect to specific functions associated with each compartment's respective share of total cellular P, N, C and Chl (Fig. 1). N is divided between the biochemical machinery of the protoplast including the cellular envelope (Q_0^N), responsible for nutrient uptake and assimilation, protein biosynthesis, much of the pigment synthesis etc., and the photosynthetic apparatus of the chloroplast ($Q^N - Q_0^N$). The protoplast also contains the nucleus and the biosynthetic apparatus and is assumed to hold all of the cell's P. P is divided between the nucleus and membranes (Q_0^P), and the biosynthetic apparatus ($Q^P - Q_0^P$), all within the protoplast, such that chloroplast P (assumed to be negligible) is subsumed as part of Q_0^P (Fig. 1). C is allocated between chloroplast and protoplast and within the protoplast according to the potential activities of each (sub-) compartment. The correspondence between these compartments and their functions and stoichiometry is of course highly simplified. The compartments must be thought of in terms of their functional equivalents in cyanobacteria.

Nutrient uptake and assimilation. Nutrient uptake and assimilation and the biosynthesis of proteins, pigments etc. mainly happen in the protoplast. Within the protoplast, N is associated with nutrient uptake and assimilation and pigment synthesis, and P is associated with protein biosynthesis. Hence, nutrient uptake activity of the protoplast can be expressed with respect to the whole cell, via the assumptions of equal N:C ratio in protoplast and chloroplast (Assumption 6) and biomass being proportional to potential activity (Assumption 7), by multiplying with the relative size (biomass fraction C_p/C) of the protoplast:

$$\frac{N_p}{C_p}=\frac{N}{C} \Leftrightarrow \frac{C_p}{C}=\frac{N_p}{N}=\frac{N_p/C}{N/C}=\frac{Q_0^N}{Q^N} \quad (8)$$

where C_p and N_p are protoplast C and N content. Nutrient uptake is based on the formulation of Aksnes & Egge (1991), where the half-saturation nutrient concentration varies as the ratio of the maximal uptake rate and affinity (V_{max}/A). P uptake is the first element in the chain of limitations (Fig. 2) and is thus described as

$$\widetilde{V^P}=\frac{Q_0^N}{Q^N}\frac{1}{V_{max}^{P\,-1}+(AP_i)^{-1}} \quad (9)$$

where P_i is ambient P concentration, $\widetilde{V^P}$ is unregulated P uptake rate and A is nutrient affinity. $\widetilde{V^P}$ will usually be the same as actual P uptake rate (V^P) but may be down-regulated if Q^P reaches its maximum (Q_{max}^P), e.g. under severe light limitation (see below).

P can be used in the same form in which it enters the cell but this is not the case for inorganic N (N_i), which, in the case of nitrate or nitrite, first has to be reduced to ammonium before it is assimilated into amino acids and finally protein. The final step, i.e. protein biosynthesis, is performed by the biosynthetic apparatus comprised of ribosomes and other forms of RNA, which

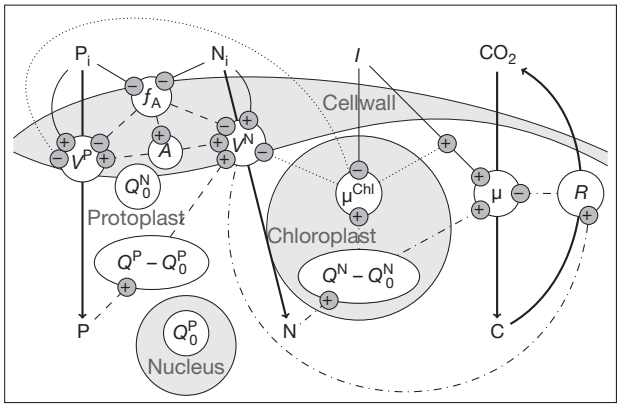

Fig. 2. Control cycles in the chain model. Nutrient assimilation and chlorophyll (Chl) dynamics constitute a chain of limitations by P, N, and light. P uptake (V^P) determines P quota (Q^P), Q^P constrains N assimilation (V^N), which in turn governs N quota (Q^N), and limits growth rate (μ) via chlorophyll synthesis (μ^{Chl}) and light harvesting. Nutrient uptake is optimised in the first control cycle (dashed lines), which balances affinity (A) against maximal P and N uptake by means of adjusting the affinity allocation factor (f_A) so as to maximise N assimilation. The second control cycle (dash-dotted lines) balances the gain in gross growth rate due to increased Q^N against respiration loss (R) incurred by nitrogen assimilation to set an upper limit for nutrient assimilation. Improved light harvesting is balanced against competing requirements for energy and enzymes between chlorophyll synthesis and nutrient assimilation in the third control cycle (dotted lines). (+) and (–) indicate positive and negative effects, respectively

have a high P content (Sterner & Elser 2002). Because chloroplast P is assumed to be negligible, cellular P is divided between nucleus and membranes (represented by Q_0^P) and the biosynthetic apparatus ($Q^P - Q_0^P$) within the protoplast, i.e. we assume P = P_p, where P_p is the protoplast P content. The relative biomass of the biosynthetic apparatus with respect to the protoplast (C_b/C_p) is calculated analogously to Eq. (8) using the above assumption of equal P:C ratio within the protoplast, as

$$\frac{P_b}{C_b}=\frac{P_p}{C_p} \;\Leftrightarrow\; \frac{C_b}{C_p}=\frac{P_b}{P_p}=\frac{P/C-P_n/C}{P/C}=1-\frac{Q_0^P}{Q^P} \quad (10)$$

where C_b and P_b are the C and P content of the biosynthetic apparatus, and P_n and P_p = P are the nucleus and protoplast (= total cellular) P content. It is assumed here for simplicity that the protoplast-normalised size (assumed proportional to its activity) of the biosynthetic apparatus, $1-\frac{Q_0^P}{Q^P}$, defines the fraction of N actually assimilated into active protein after it was taken up:

$$\widetilde{V^N}=\left(1-\frac{Q_0^P}{Q^P}\right)\frac{Q_0^N}{Q^N}\frac{1}{{V_{max}^N}^{-1}+(AN_i)^{-1}} \quad (11)$$

where $\widetilde{V^N}$ is the unregulated N assimilation rate and which is otherwise analogous to Eq. (9). Similar to $\widetilde{V^P}$, $\widetilde{V^N}$ may be down-regulated under severe light limitation to prevent above-optimal Q^N (see below).

P assimilation is assumed to be the same as P uptake, whereas some of the N taken up is lost if it cannot be assimilated. The potential N uptake capacity V_0^N can be estimated as the ratio of continuous energy turnover capacity ($D\mu_*$, see Pahlow 2005) and the amount of energy needed for N assimilation (cost of biosynthesis, ζ). Because of the assumption of an equal N:C ratio in chloroplast and protoplast and with ξ defined as the amount of C associated with each unit of Chl, fraction $\xi\theta^C$ of protoplasmic N is needed for pigment synthesis, such that fraction $1 - \xi\theta^C$ is available for nutrient uptake and assimilation, and is allocated between surface area (determining affinity A) and processing capacity (determining V_{max}^N, V_{max}^P) of the uptake apparatus (Smith & Yamanaka 2007)

$$V_0^N=\frac{D\mu_*}{\zeta} \qquad V_0^P=\frac{Q_0^P}{Q_0^N}V_0^N \quad (12)$$

$$V_{max}^N=(1-\xi\theta^C)V_0^N(1-f_A) \quad V_{max}^P=(1-\xi\theta^C)V_0^P(1-f_A) \quad (13)$$

$$A=(1-\xi\theta^C)A_0 f_A \quad (14)$$

where the affinity allocation factor f_A is the fraction of N allocated to nutrient affinity (surface area of uptake sites), A_0 is potential affinity, and V_0^N and V_0^P are potential N and P uptake capacities. The relation between V_0^N and V_0^P in the righthand Eq. (12) was chosen as the simplest possibility without introducing new parameters. Eqs. (12) to (14) describe the regulation of N distribution within the nutrient uptake apparatus by a single control cycle (of f_A) for both N and P uptake (Fig. 2).

Allocation of N between maximal uptake rates and affinity via f_A defines a control cycle for nutrient assimilation (Fig. 2). Smith & Yamanaka (2007) hypothesised that f_A should be optimised by maximising growth with respect to the limiting nutrient in a threshold formulation. Since Q^N limits growth more directly than Q^P in the chain model, the most direct strategy for maximising growth rate is to optimise total N assimilation, taking into account both the direct effect of f_A on V^N and the indirect effect mediated via V^P and Q^P. An expression for optimal f_A is thus derived from the balanced-growth approximation

$$Q^P=\frac{V^P}{V^N}Q^N=Q_0^P+r_v Q^N, \quad r_v=\frac{{V_{max}^N}^{-1}+(AN_i)^{-1}}{{V_{max}^P}^{-1}+(AN_i)^{-1}} \quad (15)$$

where V^P and V^N are actual rates of P and N assimilation. Substituting Eqs. (15), (13) & (14) into Eq. (11) and differentiating with respect to f_A gives

$$\frac{d\widetilde{V^N}}{df_A}=0 \;\Leftrightarrow\; f_A=\left[1+\sqrt{\frac{A_0\left(\frac{Q^N}{V_0^N}+\frac{Q_0^P}{V_0^P}\right)}{\frac{Q^N}{N_i}+\frac{Q_0^P}{P_i}}}\right]^{-1} \quad (16)$$

which depends on Q^N but not on Q^P. Nevertheless, f_A depends on inorganic nutrient concentrations of both N_i and P_i. We use $\widetilde{V^N}$ in Eq. (16) rather than the regulated N uptake rate V^N (see Eq. 24), as otherwise a unique f_A cannot be determined if Q^N exceeds its optimal value (Q_{opt}^N, see Eq. 23).

Gross C fixation and down-regulation of nutrient assimilation. The principal task of the chloroplast is C fixation. It contains all of the Chl and fraction $1 - Q_0^N/Q^N$ of cellular N. The assumption of equal chloroplast and protoplast N:C ratios yields a simple formula for relative chloroplast size (C_c/C), which also defines the relationship between whole cell and chloroplast Chl:C ratio (θ^C and $\hat{\theta}^C$):

$$\frac{N_c}{C_c}=\frac{N}{C} \;\Leftrightarrow\; \frac{C_c}{C}=\frac{N_c}{N}=\frac{N/C-N_P/C}{N/C}=\frac{Q^N-Q_0^N}{Q^N} \quad (17)$$

$$\Leftrightarrow\; \theta^C=\hat{\theta}^C\frac{C_c}{C}=\hat{\theta}^C\frac{Q^N-Q_0^N}{Q^N} \quad (18)$$

where C_c and N_c are chloroplast C and N content. Biomass-normalised rate of C fixation is the same as gross growth rate (μ_g), which (after Baumert 1996, Pahlow 2005) is obtained as

$$\mu_g=\mu_*\left(1-\frac{Q_0^N}{Q^N}\right)S_I, \quad S_I=1-e^{-\frac{\alpha I\hat{\theta}^C}{\mu_*}} \quad (19)$$

where S_I is the degree of light saturation of the photosynthetic apparatus and μ_* the maximum daytime rate of energy turnover. This formulation explains N limita-

tion as a restriction on the size of the photosynthetic apparatus, i.e. the N quota determines the amount of enzymes available for energy harvest and C fixation. From the fact that Q^P does not appear in Eq. (19) it follows that growth depends directly only on Q^N but not Q^P, which causes an asymmetry between the dependencies of growth on Q^N on the one hand and Q^P, mediated via Q^N, on the other.

For balanced growth, we can express the cost of biosynthesis (ζV^N) as a function of Q^N, which is substituted together with Eq. (19) in Eq. (3) to obtain an expression for growth rate averaged over 24 h.

$$\frac{V^N}{Q^N} = \frac{V^P}{Q^P} = \bar{\mu} + R_M \tag{20}$$

$$\zeta V^N = \zeta(\bar{\mu} + R_M)Q^N \tag{21}$$

$$\bar{\mu} = D\mu_* \frac{Q^N - Q_0^N}{Q^N(1+\zeta Q^N)} S_1 - R_M \tag{22}$$

where D is daylength as a fraction of 24 h. Because the increase of μ_g with Q^N saturates at high Q^N in Eq. (19) but the cost of biosynthesis increases linearly with Q^N in Eq. (21), $\bar{\mu}$ will decline as soon as Q^N increases above its optimal value (Q^N_{opt}):

$$\frac{d\bar{\mu}}{dQ^N} = 0 \quad \Leftrightarrow \quad Q^N_{opt} = Q_0^N + \sqrt{Q_0^{N^2} + \frac{Q_0^N}{\zeta}} \tag{23}$$

Thus, N assimilation should stop once Q^N_{opt} is reached to prevent super-optimal Q^N, which constitutes the second control cycle of the chain model (Fig. 2). We assume that P uptake is down-regulated in a similar manner once a maximal Q^P (Q^P_{max}, defined below) is reached:

$$V^N = \begin{cases} \widetilde{V^N} & \text{if } Q^N \le Q^N_{opt} \\ 0 & \text{if } Q^N > Q^N_{opt} \end{cases}, \quad V^P = \begin{cases} \widetilde{V^P} & \text{if } Q^P \le Q^P_{max} \\ 0 & \text{if } Q^P > Q^P_{max} \end{cases} \tag{24}$$

where V^N and V^P are actual rates of N and P assimilation. Down-regulation of N uptake was formulated as a function of $d\bar{\mu}/dQ^N$ in Pahlow (2005), which prevented Q^N from ever reaching its optimum. Eq. (24) is simpler and does not have this drawback.

Chlorophyll dynamics and model implementation. From Eq. (19), C fixation is proportional to S_I. Fraction Q_0^N/Q^N of fixed C is used in balanced growth for the protoplast and another fraction $\xi\theta^C$ is needed for the photosynthetic apparatus, leaving fraction $1 - Q^N{}_0/Q^N - \xi\theta^C$ for other purposes, such as energy required for nutrient assimilation. Increasing Q^N is beneficial for growth under most circumstances, as Q^N is usually less than Q^N_{opt}. Thus, it appears reasonable to define the control cycle for chlorophyll synthesis (Fig. 2) so as to maximise the energy available for N assimilation in balanced growth, which is proportional to $S_I(1 - Q_0^N/Q^N - \xi\theta^C)$.

If all net fixed C went into Chl synthesis, the rate of change of θ^C would be μ/ξ because ξ units of C must be used for each unit of Chl. A simple formulation for the regulation of θ^C is obtained as the product of μ/ξ and the derivative of available energy, $S_I(1 - Q_0^N/Q^N - \xi\theta^C)$, with respect to θ^C:

$$\begin{aligned} \frac{1}{\theta^C}\frac{d\theta^C}{dt} &= \frac{\mu}{\xi}\frac{d\left[S_I\left(1-\frac{Q_0^N}{Q^N}-\xi\theta^C\right)\right]}{d\theta^C} \\ &= \frac{\mu}{\xi}\frac{d\hat{\theta}^C}{d\theta^C}\frac{d\left[S_I\left(1-\frac{Q_0^N}{Q^N}\right)(1-\xi\hat{\theta}^C\right]}{d\hat{\theta}^C} \\ &= \frac{\mu}{\xi}\frac{d\left[S_I(1-\xi\hat{\theta}^C)\right]}{d\hat{\theta}^C} \\ &= \frac{\mu}{\xi}\left[\frac{\alpha I}{\mu_*}(1-S_I)(1-\xi\hat{\theta}^C) - \xi S_I\right] \end{aligned} \tag{25}$$

The minimum of Eq. (25) is $-\mu$, such that $\mu^{Chl} = 0$, in agreement with the view that down-regulation of θ^C occurs mostly via cessation of Chl synthesis rather than Chl destruction (Cullen & Lewis 1988). Eq. (25) is the same as Eq. (7) in Pahlow (2005) but was derived from an optimisation criterion at the whole cell level rather than that of the chloroplast. The steady-state solution of Eq. (25) is

$$\frac{d\theta^C}{dt} = 0 \quad \Leftrightarrow \quad \hat{\theta}^C = \frac{1}{\xi} + \frac{\mu_*}{\alpha I}\left[1 - W\left(e^{\frac{\alpha I}{\mu_*\xi}+1}\right)\right] \tag{26}$$

where W is the Lambert-W function and which maximises available energy in balanced growth.

The 4 differential Eqs. (3) to (6) comprising the chain model require specification of 8 model parameters, A_0, α, μ_*, Q_0^N, Q_0^P, R_M, ξ and ζ. ζ may be calculated from theoretical considerations and daylength effects can be included with one additional parameter. Implementing the chain model dynamically involves 4 steps; Step 1: calculate Q^P, Q^N, θ^C from C, N, P, Chl; Step 2: calculate $\hat{\theta}^C$ and f_A according to Eqs. (16) & (18); Step 3: calculate V^P, V^N, μ^{Chl}, μ according to Eqs. (24), (19), (25) & (3); and Step 4: calculate the rates of change defined in Eqs. (3) to (6). N_i and P_i are obtained from mass balance in a closed system and the 2 additional differential equations required for an open system are readily derived.

Balanced growth and limit behaviour. The 2 most common situations where steady-state solutions are needed are simulations of chemostat and turbidostat experiments. Chemostat cultures are usually considered nutrient limited because nutrients are often depleted to undetectable levels, whereas turbidostats are considered light limited because nutrient concentrations remain high in the culture vessels in these experiments. It follows from Eq. (26) that the chloroplast Chl:C ratio $\hat{\theta}^C$ (and hence S_I) is only a function of

irradiance in balanced growth. In a chemostat, the growth rate is set by the dilution rate, thus $\bar{\mu}$ is known and Q^N can be calculated from S_I and Eq. (22). N_i, P_i and Q^P can then be obtained using the additional constraint

$$\frac{Q^N}{Q^P} = \frac{N_t - N_i}{P_t - P_i} \tag{27}$$

where N_t and P_t are the N and P concentrations in fresh culture medium. The solution of Eq. (27) is given in Appendix 1. In a turbidostat, N_i and P_i are known and Q^N is obtained as the solution of Eqs. (20) & (22), which is also given in Appendix 1. The turbidostat solution might also be convenient for use in biogeochemical models, where it could be used to reduce the number of tracers, as only the inorganic nutrient concentrations and one of cellular C, N, or P are needed to define steady-state phytoplankton growth rate and composition.

The behaviour at extreme light limitation is trivial as Eq. (24) ensures that

$$\lim_{I\to 0} Q^N = Q^N_{opt} \tag{28}$$

which applies to zero growth rate for negligible maintenance respiration and hence negligible compensation irradiance. Under extreme nutrient limitation, Q^N approaches Q^N_0 only for negligible maintenance respiration. Otherwise the lower limit of Q^N is obtained from Eq. (22) as:

$$\lim_{\bar{\mu}\to 0} Q^N = \frac{1}{2\zeta}\left(\frac{D\mu_* S_I}{R_M} - 1\right) - \sqrt{\frac{1}{4\zeta^2}\left(\frac{D\mu_* S_I}{R_M} - 1\right)^2 - Q^N_0 \frac{D\mu_* S_I}{\zeta R_M}} \tag{29}$$

The highest growth rate is achieved when both nutrient concentrations and irradiance are saturating. Under these conditions, we obtain from Eqs. (15), (20), & (22):

$$\lim_{\substack{N_i\to\infty \\ P_i\to\infty \\ I\to\infty}} Q^N = \frac{Q^N_0}{2} + \sqrt{1.25(Q^N_0)^2 + \frac{Q^N_0}{\zeta}} \tag{30}$$

$$\lim_{\substack{N_i\to\infty \\ P_i\to\infty}} Q^P = Q^P_0\left(1 + \frac{Q^N}{Q^N_0}\right) \tag{31}$$

Eq. (31) defines Q^P if both N_i and P_i are saturating and is valid irrespective of I. Consequently, variability of Q^P is greater than that of Q^N. Substituting Q^N_{opt} for Q^N in Eq. (31) should thus provide a reasonable (although somewhat arbitrary) estimate for the maximum of Q^P (Q^P_{max}):

$$Q^P_{max} = Q^P_0\left(1 + \frac{Q^N_{opt}}{Q^N_0}\right) \tag{32}$$

The ratio Q^N_{opt}/Q^P_{max} is the cellular N:P ratio in the absence of nutrient limitation.

Steady-state model behaviour under typically encountered (experimental) conditions is outlined in Fig. 3. For nutrient limitation, the model displays a striking asymmetry between P:C and N:C behaviour (Fig. 3A, B): P:C behaviour depends strongly on input N:P, whereas N:C shows a unique relationship to growth rate, which is of course a consequence of μ_g being only a function of N in Eq. (19). The difference between the dashed and solid curves in Fig. 3B is due to the difference in μ_{max}. The outermost (solid or dashed) curves in Fig. 3C delimit the region of colimitation, where growth rate is affected by both N and P. Growth is N limited below and P limited above the region of colimitation in Fig. 3C. Horizontal straight segments within the region of colimitation indicate that $N:P \approx N_t:P_t$ because N and P are almost completely utilised by the algae. Growth is purely N limited at N:P supply ratios below and purely P limited above this region. The extent of the region of colimitation depends on actual nutrient concentration (Fig. 3C, dashed and solid lines), as does the overall shape of the predicted relationship between N:P ratio and growth rate. Cell N:P will track input N:P ratio throughout much of the range of experimental conditions for nutrient limitation (Fig. 3C, solid lines), with substantial deviations only at extreme N:P input ratio or relatively high growth rate. However, deviations between cell N:P and supply N:P ratio increase with decreasing nutrient concentrations (Fig. 3C, dashed lines).

An asymmetry between P:C and N:C behaviour is also predicted, albeit less clearly, under light-limited conditions (Fig. 3D,E). The P:C ratio decreases similarly throughout the whole range of growth rates with decreasing P_i concentration, whereas N:C varies much less at low than at high growth rate (irradiance). The small variation in N:C at zero growth rate in Fig. 3E indicates non-negligible compensation irradiance, which is due to maintenance respiration. N:C variability is most pronounced at low nutrient concentration and both N:C and P:C are affected about as much by absolute nutrient concentration as N:P supply ratio. N:P variability consequently depends strongly on absolute nutrient concentration and is strongest with low light and low (realistic) nutrient concentration (Fig. 3F). In contrast to nutrient limitation, light limited N:P is thus closer to $N_t:P_t$ at lower nutrient concentrations.

RESULTS

Figs. 4 to 8 compare model predictions with experimental observations. Model parameters were adjusted by hand to obtain as good as possible an agreement between model and observations (based on normalised residual sums of squares), except that ζ, the cost of biosynthesis coefficient, was calculated as described in

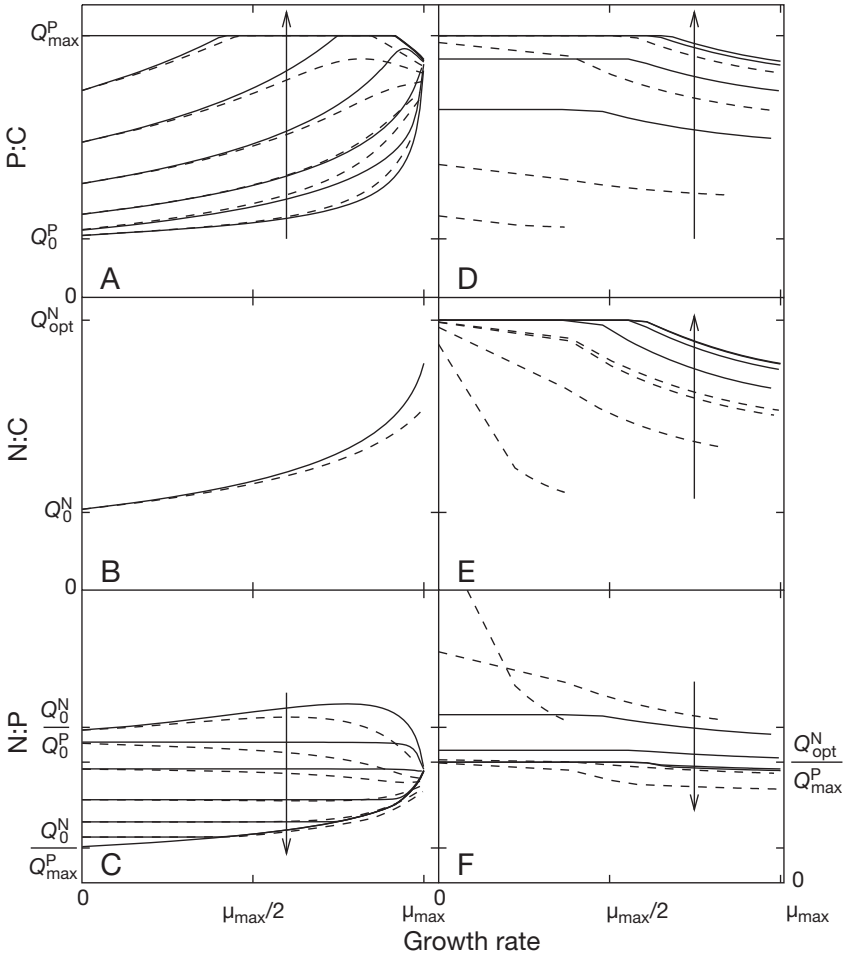

Fig. 3. Stable steady-state behaviour of modelled cell quotas and N:P ratio under nutrient (A–C) and light limitation (D–F). Vertical arrows indicate direction of increasing inorganic P concentration. Solid lines are for N_t = 500 µM (μ_{max} = 1.34 d^{-1}), dashed lines are for N_t = 30 µM (μ_{max} = 1.25 d^{-1}). N_t:P_t ratios range from 100 to 5 (panels A–C) and from 5000 to 16.7 (panels D–F). Corresponding dashed and solid lines are for the same N_t:P_t ratios

Pahlow (2005). Fig. 4 most clearly shows the unique relationship between nutrient limited growth rate and N:C ratio (Fig. 4A) predicted by the model and observed by Laws & Bannister (1980). Similar unique relationships can be seen also for Chl:C and Chl:N ratios (Fig. 4C,D). The slope in P limited N:P ratio (Fig. 4B) indicates significant unused N_i (cf. topmost line in Fig. 3C), which is also clear from the fact that cell N:P is much lower than the input N:P ratio. The remaining curves and points ascertain the overall consistency of the model with this dataset.

Fig. 5 shows a somewhat different behaviour in that the P limited N:C ratio deviates from the N limited N:C ratio at the lowest growth rate in data from Terry et al. (1985). Consequently, the N:P ratio becomes very high (Fig. 5 A,B). However, the deviation in N:C is about the same as for ammonium limitation in Fig. 4A, and the N_i source used by Terry et al. (1985) was also ammonium. Hence, it remains unclear whether the difference between the N and P limited N:C ratio at low growth rate could be ascribed to the nature of the limiting element or to increased variability due to the use of ammonium as the N_i source. Nevertheless, with the exception of the lowest P limited growth rate, these data support a unique relationship between the N:C ratio and a nutrient limited growth rate. Conversely, the P:C ratio exhibits 2 very distinct patterns under N and P limitation (Fig. 5C), which demonstrates the asymmetry of non-limiting nutrient quota between N and P limitation.

The dataset by Healey (1985) for *Synechococcus linearis* was the most complete we could find (Figs. 6 & 7). Greater discrepancies between model and observations could be expected for *S. linearis*, as (1) being a freshwater species, it lives in a very different environment than the organisms discussed above, and (2) being a cyanophycean, it also has a very different cellular organisation. With the exception of total biomass concentration and N:P ratio under severely P limited conditions (Fig. 7A,F), however, the model fits the data fairly well. The asymmetry between N:C and P:C, in particular, is clearly born out in this dataset: N:C ratio behaves similarly, albeit not quite the same, under both N and P limitation (Figs. 6B & 7B), whereas P:C displays a hyperbolic relationship to growth rate only under P limiting conditions (Figs. 6C & 7C). Chl:C and Chl:N clearly follow the same pattern for N and P limitation, which is distinct from that observed for light limitation (Figs. 6E,F & 7D,E).

Fig. 8 shows the behaviour of the freshwater green alga *Scenedesmus* sp. over a wide range of N_t:P_t ratios. The model predicts that Chl:C and N:C should be independent of N_t:P_t and this seems to be the case for Chl:C. N:C appears to be increasing at high N_t:P_t ratios, but only the N:C ratio corresponding to the highest N_t:P_t of 80 is clearly outside the range encompassed for N_t:P_t < 50 (Fig. 8A). Cell N:P simply tracks N_t:P_t in this experiment, whereas the model predicts a lower limit of about 10 and an upper limit of about 47 (Fig. 8B). Predicted biomass build-up closely matches the observations (Fig. 8B).

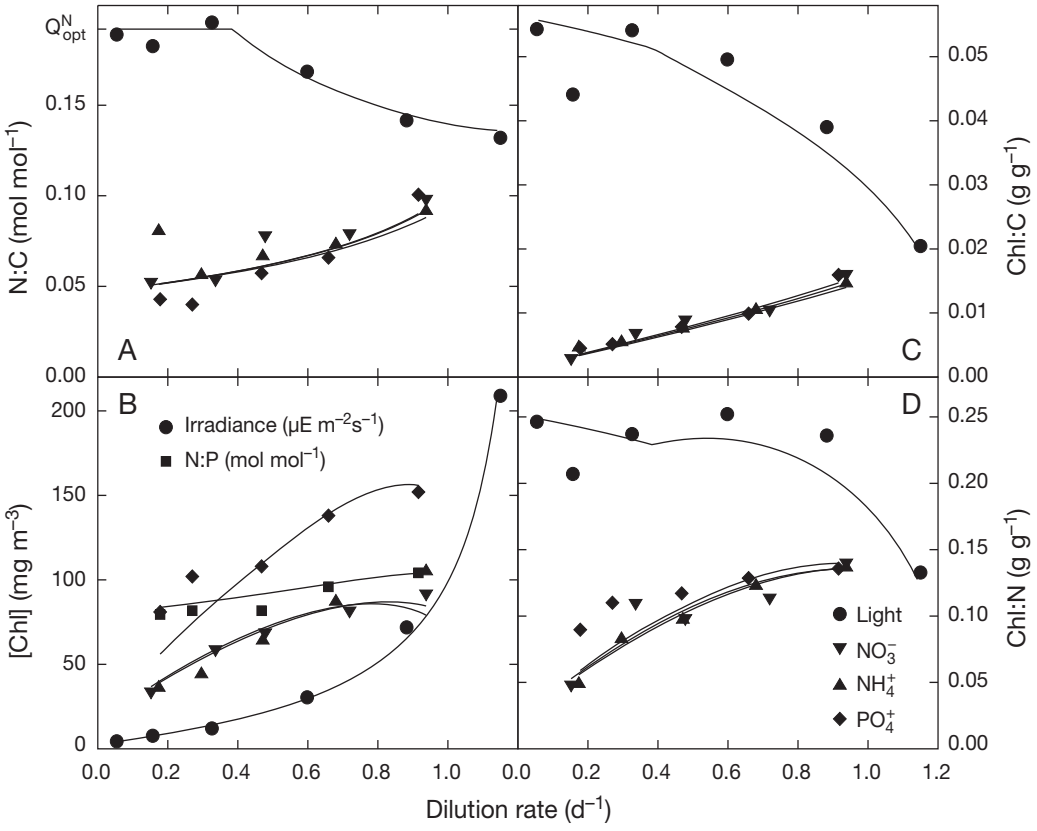

Fig. 4. *Thalassiosira fluviatilis*. Elemental composition and total Chl concentration under light (N_t:P_t = 4.25), N (N_t:P_t =1) and P (N_t:P_t = 266) limited quasi steady state conditions. Symbols are observations and solid lines are model predictions. Closed circles in (C) indicate the relationship between light limited growth rate and irradiance. N:P ratio for P limited experiments (squares in B) was estimated from observed N and predicted P (≈ P_t). Data from Laws & Bannister (1980, 2004). Parameter definitions in Table 2

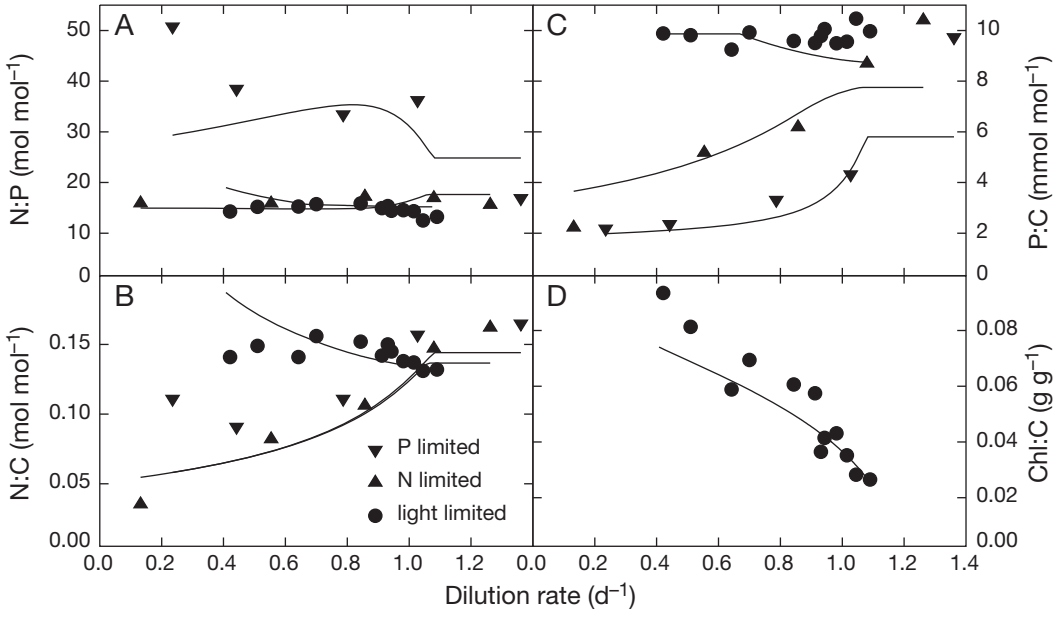

Fig. 5. *Phaeodactylum tricornutum*. Elemental composition in growth limited by P (N_t:P_t = 75), N (N_t:P_t = 15) and light (N_t:P_t = 6). Data from Terry et al. (1983, 1985)

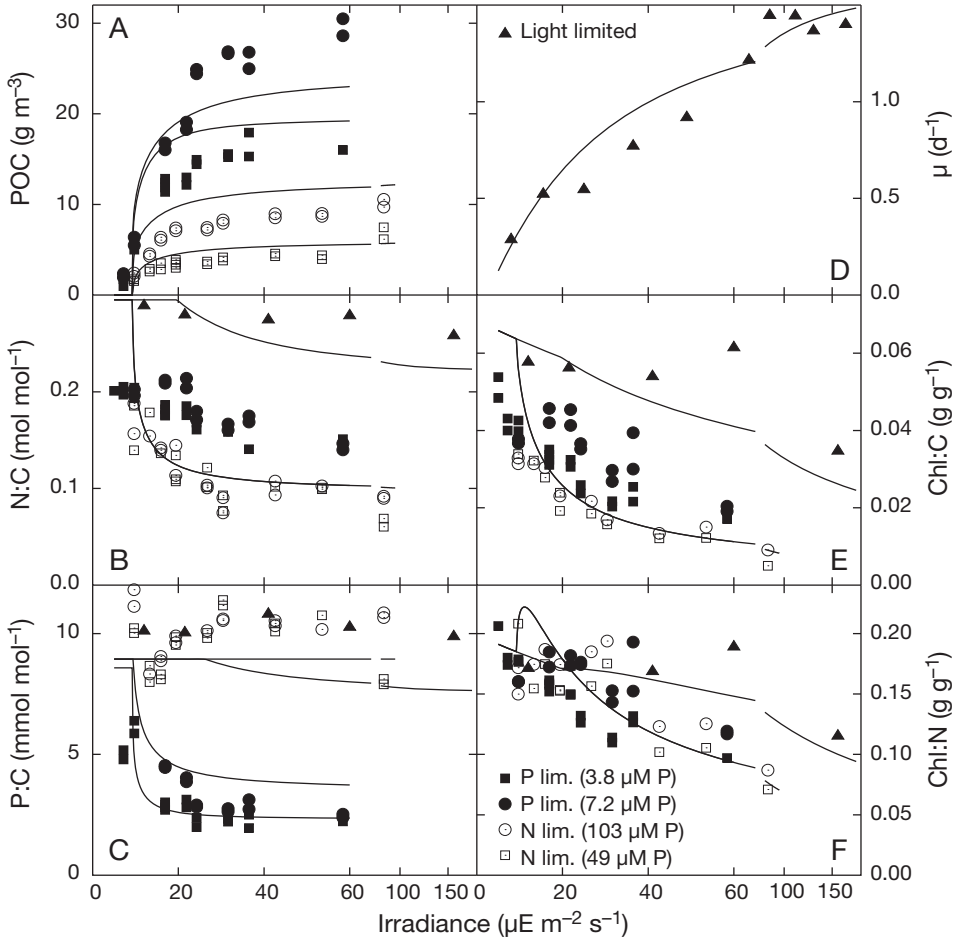

Fig. 6. *Synechococcus linearis*. Growth under light, N and P limited conditions. Nutrient limited experiments are for a constant growth rate of 0.31 d^{-1}. Data from Healey (1985). Parameters in Table 2

Thus, it appears that the model was able to reproduce the observations from the different experiments with varying success. However, discrepancies between model and data are not greater than discrepancies among the experiments. For example, the high N:P seen in Fig. 8B matching the input N:P ratio is not reproduced by the model for input N:P > 50, but this behaviour is also not seen in Fig. 4B for an input N:P ratio of 266, where the model describes the data correctly. Similarly, Figs. 4A & 6B show declining N:C ratio with increasing irradiance for light limitation, as predicted by the model, whereas such a decline is absent in Fig. 5B.

Our parameter estimates for Q_0^P are between 0.0012 and 0.002. Sterner & Elser (2002) estimate the contribution of P contained in DNA to total Q^P in zooplankton to be about 0.0013, with a similar contribution from phospholipids. Geider & La Roche (2002) report biomass contributions (in g gC^{-1}) of DNA and phospholipids in phytoplankton as 0.5 to 3% and 5 to 15%, giving contributions to total Q^P of 0.0005 to 0.003 molP molC^{-1} and 0.0013 to 0.004 molP molC^{-1}, respectively. These ranges overlap with our estimates for Q_0^P and thus illustrate that above interpretation for Q_0^P is consistent with current thinking about plankton stoichiometry.

DISCUSSION

The most conspicuous difference between our chain model and other models of multi-nutrient limitation (e.g. Flynn 2001, 2008, Klausmeier et al. 2004b, Smith & Yamanaka 2007) are the invariance of the relationship between a nutrient limited growth rate and the N:C ratio predicted by Eq. (22), and the resulting strong asymmetry between the cell quotas of the respective non-limiting nutrients. Flynn (2008) generated an asymmetry between non-limiting N:C and P:C by means of adding different multipliers for non-limiting N and P transport, whereas the asymmetry follows naturally from the structure of the chain model presented here. The asymmetry

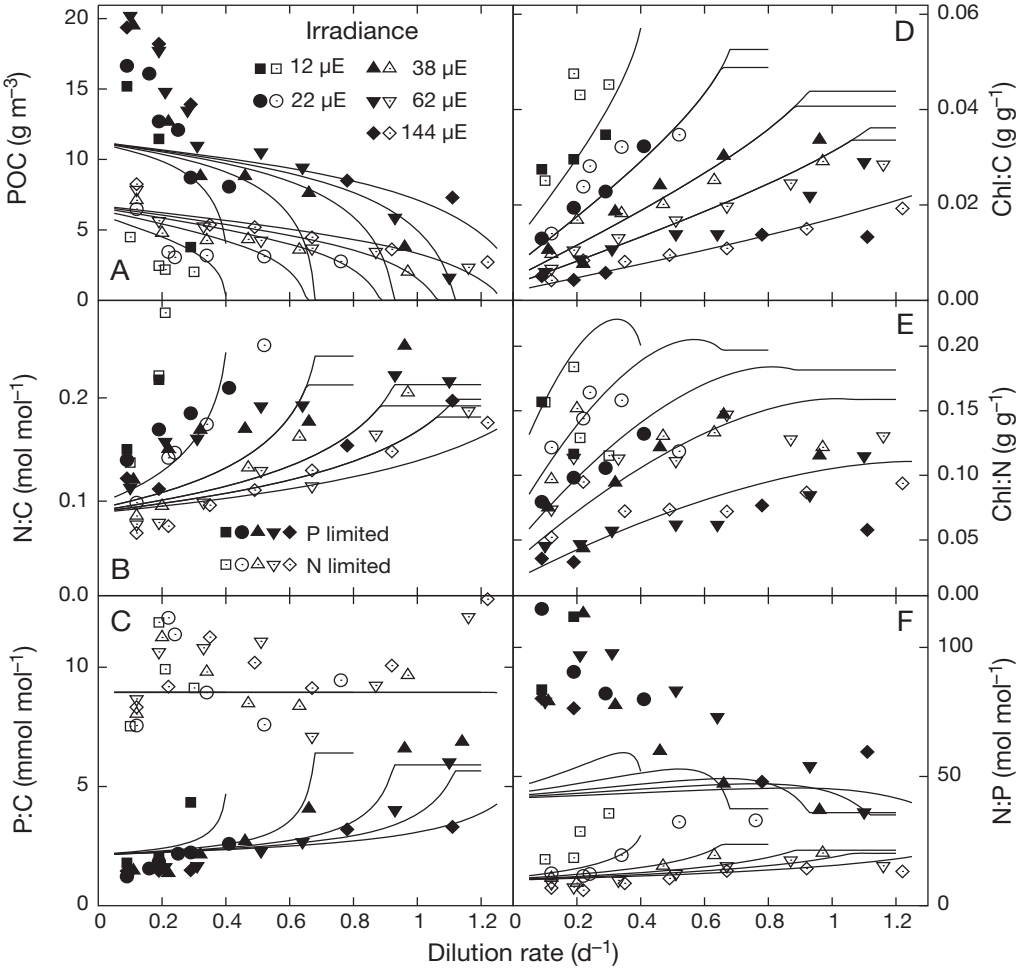

Fig. 7. *Synechococcus linearis*. Transition from N or P to light limited conditions. Data from Healey (1985). Parameter definitions in Table 2

between N:C and P:C behaviour seems to be a general phenomenon evident in all observations shown above. The invariance of the N:C vs. growth relationship appears to hold for a wide range of growth conditions, but N:C can also increase under P limitation, particularly with ammonium as the N source or at very high input N:P ratios (e.g. Figs. 5B, 6B & 8A). Nevertheless, the model still reproduces Chl:C ratios and, except for the lowest growth rates in Fig. 7A, also biomass accumulation in these cases. The slight increase in non-limiting N:C under strong P limitation would agree better with the Flynn (2008) model, which, however, cannot reproduce the unique relation between N:C and growth shown in Fig. 4A (see Fig. 1 in Flynn 2008).

The chain model assumes that all assimilated N contributes to enzyme activity, where a fixed amount relative to biomass is reserved for protoplast activity Q_0^N and the (variable) remainder is available for the chloroplast and determines Chl:C according to Eq. (18). In spite of the variations with N:P supply ratio in the N:C vs. growth relationship seen in Figs. 5B, 6B & 8A, no such variations are evident for the Chl:C vs. growth relationship (Figs. 6E, 7D & 8A). As the model describes optimal growth and predicted N:C suffices to produce the observed levels of C and Chl, the difference between observed and modelled N:C could be interpreted as luxury or storage N assimilation in the context of the chain model. In this case however, growth would not be optimal as the storage fraction of cell N would contribute to N assimilation costs but not to enzyme activity. In this respect, the lower cost associated with ammonium as compared to nitrate assimilation might also explain why such storage N assimilation might occur for N limitation in Fig. 4A and P limitation in Fig. 5B with ammonium as N_i source, but not for P limitation (with the highest input N:P ratio) with nitrate as N_i source in Fig. 4A.

The model underestimates biomass build up under severe P limitation for the cyanophycean shown in Fig. 7A, although chlorophyll and biomass appear to

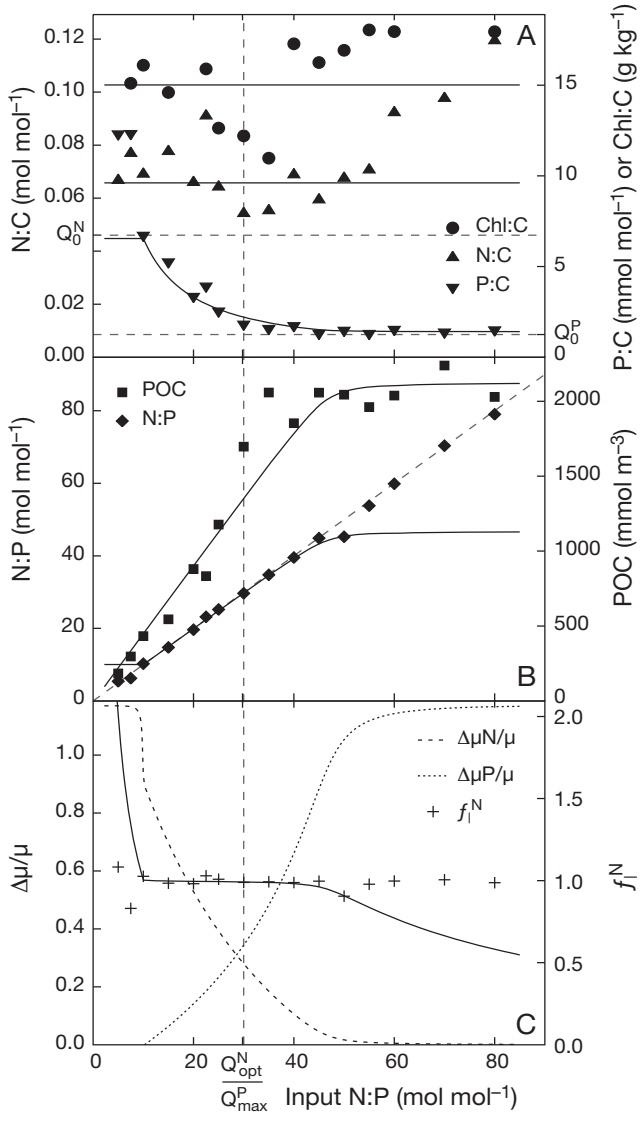

Fig. 8. *Scenedesmus* sp. Transition from N to P limitation at constant growth rate (0.59 d^{-1}). Dashed horizontal lines in (A) indicate Q_0^N and Q_0^P. Q_{opt}^N is 0.19 mol mol^{-1} with the parameters for this experiment (Table 2). Dashed vertical line denotes $N_t:P_t = 30$, marking the transition point from N to P limitation determined by Rhee (1978), and dashed diagonal line in (B) is the 1:1 line. Biomass was calculated from rate of C fixation $cell^{-1}$ divided by 0.59 d^{-1} or from cell volume. Relative growth rate increments $\frac{\Delta\mu_N}{\mu}$ and $\frac{\Delta\mu_P}{\mu}$ in (C) indicate the degree of limitation by N and P, respectively, and were obtained by setting the respective ambient nutrient concentrations to saturating levels (10 µM [PO_4] and 300 µM [NO_3]) and recalculating growth rate as the steady-state solution to Eqs. (20) & (22) given by Eqs. (A7) to (A 11). Values close to 1 in the relative utilisation index ($f_I^N \approx 1$ in panel C) mark the region of colimitation. Data from Rhee (1978)

be correctly described for other (eukaryotic) species (Figs. 4B & 8B). The high biomass observed for the cyanophycean could be related to the ability of these organisms to reduce their P requirement under P stress by replacing phospholipids with sulfolipids (Van Mooy et al. 2006). This interpretation is supported by an apparent step in P limited P:C in Fig. 7C: For growth rates above 0.4 d^{-1} the lowest P:C ratio is about 2 mmol mol^{-1}, whereas it is only half this value for lower growth rates; consequently, biomass (determined by C:P) is also underestimated by up to 50%.

Growth limitation by N and P was classified as independent (type I) colimitation by Saito et al. (2008), referring to the results of Rhee (1978), who interpreted the dataset shown in Fig. 8 as evidence for the absence of interactions between growth limiting effects of N and P on the grounds that (1) the sharp transitions in cellular C, N, and P content at the transition between N and P limitation were inconsistent with colimitation effects, and (2) the (symmetrical) multiplicative model was rejected by statistical analysis. Firstly, abrupt transitions are not visible close to the transition point between N and P limitation for biomass-normalised cell quotas (N:C = Q^N and P:C = Q^P) in Fig. 8, which can be thought of as a vertical cut through Fig. 3A to C. The transition point was estimated by Rhee (1978) at $N_t:P_t$ = 30, which matches the predicted value of Q^N_{opt}/Q^P_{max} = 29.8. The sharp transitions for cellular N and P content reported by Rhee (1978) were accompanied by concomitant changes in C, which resulted in the smooth behaviour of Q^N and Q^P around the transition point in Fig. 8. Thus, the consistency between the (colimitation) model and observations around the transition point indicates that sharp transitions on a per cell basis do not contradict colimitation effects.

Secondly, a multiplicative cell-quota model is not the only way to describe colimitation. Indeed, the good agreement between the chain (colimitation) model and observed N:P for input N:P ratios from 10 to 50 in this experiment means that these data do not contradict colimitation by N and P. On the contrary, the increase in biomass accumulation with increasing input N:P ratio for P limitation, i.e. beyond the optimal N:P of 30 Rhee (1978), could actually be taken as evidence for colimitation. Considering P limitation as a restriction of the ability to assimilate N implies classifying N and P limitation as biochemically dependent colimitation (Arrigo 2005, Saito et al. 2008). This interpretation would also explain the frequent but irregular observation of growth stimulation by individual additions of N and P (co-stimulation, Flemer et al. 1998), which would not be expected if only one nutrient was limiting. Other explanations for this phenomenon, such as relief of grazing pressure, suffer from the absence of a clear relationship between experimental setup and the occurrence of co-stimulation.

The chain model describes colimitation by light, N, and P, which it has in common with multiplicative cell-quota models, while also providing a clearly-defined transition point between N and P limitation, which is

typical of threshold formulations. The transition point at N:C = Q^N_{opt}/Q^P_{max} defines N and P limitation with respect to cellular composition. It is often desirable to determine the limiting nutrient from measurements of inorganic (external) and cellular (internal) nutrient concentrations without exact knowledge of Q^N_{opt} and Q^P_{max}. The chain model can be used to define the external limiting nutrient operationally but precisely as that nutrient which is utilised preferentially, i.e. in a higher proportion than at which it is supplied, and which can be quantified by means of a relative utilisation index for N ($f_1{}^N$) as

$$f_1^N = \frac{V^N : V^P}{N_t : P_t} \approx \frac{N:P}{N_t : P_t} \quad (33)$$

If $f_1{}^N > 1$ N is the limiting nutrient, $f_1{}^N < 1$ indicates P limitation and if $f_1{}^N \approx 1$ (i.e. when N:P matches the input ratio), N and P are both limiting. This definition could be invalid if the cells stored N or P in an inactive pool or otherwise tracked the input N:P ratio as shown in Fig. 8B, C, but this behaviour appears to be an exception rather than the rule (Hall et al. 2005) and is not evident in the other datasets discussed here either. The definition of the relative utilisation index could easily be extended to more than 2 nutrients: By taking 1 nutrient as a reference and then calculating relative utilisation indices for each nutrient with respect to the reference nutrient, one could thus establish the relative importance of each nutrient for overall growth limitation.

We find $f_1{}^N \approx 1$ throughout much of the region of colimitation in Fig. 3C, particularly when high inorganic nutrient concentrations are used in the input medium (horizontal solid lines in Fig. 3C). $f_1{}^N$ could hence be used to determine whether phytoplankton growth is colimited or limited by only one nutrient in chemostat experiments. Limitation by one element applies only if $f_1{}^N$ is clearly different from 1, which will only occur if a significant remnant concentration of the non-limiting element is detected in the culture vessel. The relative utilisation index is applied to the data by Rhee (1978) together with predicted relative growth rate increments in Fig. 8C. The region of colimitation is defined by significant effects of both N and P on growth rate, i.e. $\frac{\Delta\mu_N}{\mu} > 0$ and $\frac{\Delta\mu_P}{\mu} > 0$, and spans input N:P ratios roughly from 10 to 50, which is the same range where $f_1{}^N \approx 1$. Thus, transition from N to P limitation occurs over a rather wide region of colimitation rather than a sharply-defined transition point.

In a nutrient limited (chemostat) experiment, phytoplankton biomass increases initially until (limiting) nutrients are nearly used up. Phytoplankton blooms behave very similarly in that they end when nutrients are more or less exhausted. Thus, it appears possible to interpret the findings relating cell N:P to supply N:P ratios with respect to the Redfield N:P ratio. Fig. 3C, F shows that N:P can vary strongly for light limitation but deviates only relatively little in nutrient limited experiments, where the relative utilisation index would be close to 1 in most cases. From the parameter estimates in Table 2, $Q^N_0{:}Q^P_0$ is about 35 to 40, the transition point Q^N_{opt}/Q^P_{max} is about 30 to 35, and the lowest light limited N:P in Fig. 3F is 20 to 30, which is still much higher than the Redfield N:P. Geider & La Roche (2002) also reported a transition from N to P limitation for N:P supply ratios between 20 and 50. If the species considered in the present study are representative, inorganic N and P supply in Redfield proportions from the deep ocean could thus appear to cause N limitation of marine primary production. However, the almost complete exhaustion of both N and P indicates that $f_1{}^N \approx 1$ and, therefore, the transition point is of little significance and primary production should be considered to be colimited by N and P.

Considering optimal allocation between cellular resource acquisition and assembly machinery, Klausmeier et al. (2004a) found that Redfield N:P in phytoplankton is not optimal. Instead, it results from averaging N:P ratios from species adapted to different growth conditions that just happen to occur in the right proportions to match

Table 2. Parameter settings for Figs. 4 to 8

Parameter	*Thalassiosira pseudonana*	*Phaeodactylum tricornutum*	*Synechococcus linearis*	*Scenedesmus* sp.	Units
A_0	0.12	0.16	0.1	0.25	m^3 (mmol C d)$^{-1}$
α	2.29	0.81	1.685	0.29	10^{-5} m^2 gC (µE g Chl)$^{-1}$
μ_*	5.4	4.85	4.42	10.0	d^{-1}
Q^N_0	0.045	0.05	0.085	0.046	mol N (mol C)$^{-1}$
Q^P_0	0.00124	0.0018	0.002	0.00125	mol N (mol C)$^{-1}$
R_M	0.1	0.031	0.14	0.086	d^{-1}
ξ	6.67	4.44	5.2	9.0	g C (g Chl)$^{-1}$
ζ	1.8/2.3[a]	1.8	2.3	2.3	mol C (mol N)$^{-1}$

[a]1.8 for ammonium, 2.3 for nitrate, see Pahlow (2005)

deep ocean N_i:P_i. Thus, phytoplankton N:P can change over time. The chain model predicts that phytoplankton can optimise growth by almost complete utilisation of both N_i and P_i across a wide range of N:P supply ratios (region of colimitation in Fig. 3C). Hence, in contrast to the results of Klausmeier et al. (2004a), the close match between phytoplankton and Redfield N:P ratios in the ocean is predicted to result from optimal utilisation of N and P. Nevertheless, the chain model concurs with the predictions that the Redfield N:P is not necessarily the optimal N:P ratio and that the average plankton N:P ratio might change over time.

Acknowledgements. We thank I. Hense and K.W. Wirtz for helpful comments on the manuscript. Constructive comments of 2 anonymous reviewers greatly improved the manuscript.

LITERATURE CITED

Ågren GI (2004) The C:N:P stoichiometry of autotrophs — theory and observations. Ecol Lett 7:185–191

Aksnes DL, Egge JK (1991) A theoretical model for nutrient uptake in phytoplankton. Mar Ecol Prog Ser 70:65–72

Armstrong RA (1999) An optimization-based model of iron-light-ammonium colimitation of nitrate uptake and phytoplankton growth. Limnol Oceanogr 44:1436–1446

Armstrong RA (2006) Optimality-based modeling of nitrogen allocation and photoacclimation in photosynthesis. Deep-Sea Res II 53:513–531

Arrigo KR (2005) Marine microorganisms and global nutrient cycles. Nature 437:349–355

Baumert H (1996) On the theory of photosynthesis and growth in phytoplankton. Part I: Light limitation and constant temperature. Int Rev Gesamten Hydrobiol 81: 109–139

Cullen JJ, Lewis MR (1988) The kinetics of algal photoadaptation in the context of vertical mixing. J Plankton Res 10:1039–1063

Droop MR (1973) Some thoughts on nutrient limitation in algae. J Phycol 9:264–272

Flemer DA, Livingston RJ, McGlynn SE (1998) Seasonal growth stimulation of sub-temperate estuarine phytoplankton to nitrogen and phosphorus: An outdoor microcosm experiment. Estuaries 21:145–159

Flynn KJ (2001) A mechanistic model for describing dynamic multi-nutrient, light, temperature interactions in phytoplankton. J Plankton Res 23:977–997

Flynn KJ (2008) The importance of the form of the quota curve and control of non-limiting nutrient transport in phytoplankton models. J Plankton Res 30:423–438

Geider RJ, La Roche J (2002) Redfield revisited: variability of C:N:P in marine microalgae and its biochemical basis. Eur J Phycol 37:1–17

Geider RJ, MacIntyre HL, Kana TM (1998) A dynamic regulatory model of phytoplanktonic acclimation to light, nutrients, and temperature. Limnol Oceanogr 43:679–694

Hall SR, Smith VH, Lytle DA, Leibold MA (2005) Constraints on primary producer: stoichiometry along: supply ratio gradients. Ecology 86:1894–1904

Healey FP (1985) Interacting effects of light and nutrient limitation on the growth rate of *Synechococcus linearis* (Cyanophyceae). J Phycol 21:134–146

Klausmeier CA, Litchman E, Daufresne T, Levin SA (2004a) Optimal nitrogen-to-phosphorus stoichiometry of phytoplankton. Nature 429:171–174

Klausmeier CA, Litchman E, Levin SA (2004b) Phytoplankton growth and stoichiometry under multiple nutrient limitation. Limnol Oceanogr 49:1463–1470

Laws EA, Bannister TT (1980) Nutrient and light limited growth of *Thalassiosira fluviatilis* in continuous culture, with implications for phytoplankton growth in the ocean. Limnol Oceanogr 25:457–473

Laws EA, Bannister TT (2004) Erratum: Nutrient and light limited growth of *Thalassiosira fluviatilis* in continous culture, with implications for phytoplankton growth in the ocean. Limnol Oceanogr 49:2316

Laws EA, Chalup MS (1990) A microalgal growth model. Limnol Oceanogr 35:597–608

Laws EA, Wong DCL (1978) Studies of carbon and nitrogen metabolism by 3 marine phytoplankton species in nitrate-limited continuous culture. J Phycol 14:406–416

Pahlow M (2005) Linking chlorophyll-nutrient dynamics to the Redfield N:C ratio with a model of optimal phytoplankton growth. Mar Ecol Prog Ser 287:33–43

Rhee GY (1978) Effects of N:P atomic ratios and nitrate limitation on algal growth, cell compositions, and nitrate uptake. Limnol Oceanogr 23:10–25

Saito MA, Goepfert TJ, Ritt JT (2008) Some thoughts on the concept of colimitation: Three definitions and the importance of bioavailability. Limnol Oceanogr 53:276–290

Shuter B (1979) A model of physiological adaptation in unicellular algae. J Theor Biol 78:519–552

Smith SL, Yamanaka Y (2007) Optimization-based model of multinutrient uptake kinetics. Limnol Oceanogr 52: 1545–1558

Sterner RW, Elser JJ (2002) Ecological stoichiometry: the biology of elements from molecules to the biosphere. Princeton University Press, Princeton, NJ

Terry KL (1980) Nitrogen and phosphorus requirements of *Pavlova lutheri* in continuous culture. Bot Mar 23: 757–764

Terry KL, Hirata J, Laws EA (1983) Light-limited growth of two marine strains of the marine diatom *Phaeodactylum tricornutum* Bohlin: Chemical composition, carbon partitioning, and the diel periodicity of physiological processes. J Exp Mar Biol Ecol 68:209–227

Terry KL, Hirata J, Laws EA (1985) Light-, nitrogen-, and phosphorus-limited growth of *Phaeodactylum tricornutum* Bohlin strain TFX-1: chemical composition, carbon partitioning, and the diel periodicity of physiological processes. J Exp Mar Biol Ecol 86:85–100

Van Mooy BAS, Rocap G, Fredricks HF, Evans CT, Devol AH (2006) Sulfolipids dramatically decrease phosphorus demand by picocyanobacteria in oligotrophic marine environments. Proc Natl Acad Sci USA 103:8607–8612

Appendix 1. Steady-state solutions

In a nutrient limited (chemostat) steady state $\bar{\mu}$ is given by the dilution rate and Q^N can be calculated from (22). Hence, V^N and f_A are also known and we can make use of Eqs. (16) & (27) to obtain:

$$\frac{Q^N}{N_i} + Q_0^P/P_i = A_0 A', \quad A' = \left(\sqrt{\frac{Q_0^N(1-\xi\theta^C)}{V^N}} - \sqrt{\frac{Q^N}{V_0^N} + \frac{Q_0^P}{V_0^P}} \right)^2 \tag{A1}$$

Substituting Eq. (A1) for P_i in Eq. (27) gives Q^P as a function of N_i, which is substituted into Eq. (11) to produce a cubic equation in N_i, which was solved analytically:

$$X' = A_0 f_A \left[\left(\frac{Q^N V^N}{(1-f_A)V_0^N} - (1-\xi\theta^C)Q_0^N \right)(A_0 A' P_t - Q_0^P) + (A_0 A' P_t - Q_0^P) Q_0^N Q_0^P \left(\frac{A_0 A' N_t}{Q^N} + 1 \right) \right] \tag{A2}$$

$$Y' = V^N \left[Q^N (A_0 A' P_t - Q_0^P) - \frac{A_0 f_A P_t Q^{N^2}}{(1-f_A)V_0^N} - A_0 f_A (1-\xi\theta^C) Q_0^N (N_t Q_0^P - P_t Q^N) \right. \tag{A3}$$

$$Z' = A_0^2 A' f_A (1-\xi\theta^C) Q_0^N Q_0^P \tag{A4}$$

$$N_i = 2\cos\left\{ \frac{1}{3} \operatorname{acos} \frac{\sqrt{6.75}\left[\left(Y' + \frac{2Q^N X'^2}{9Z'} \right) \frac{X'}{3} - P_t V^N Q^N Z' \right]}{\frac{Q^N}{Z'} \left(\frac{X'^2}{3} + \frac{Y'Z'}{Q^N} \right)^{1.5}} \right\} \cdot \sqrt{\left(\frac{Q^N X'}{3Z'} \right)^2 + \frac{Q_0^N Y'}{3Z'}} + \frac{Q^N X'}{3Z'} \tag{A5}$$

If the solution violates one or both of the obvious constraints

$$N_i < N_t \quad \text{and} \quad P_i < P_t \tag{A6}$$

the dilution rate exceeds the maximal predicted growth rate (washout) and the solution must be obtained for light limited conditions using Eqs. (A8) to (A10) with $N_i = N_t$ and $P_i = P_t$.

The light limited (turbidostat) steady state solution is obtained numerically with the help of Eqs. (20), (22) & (16). Substituting Eqs. (11) & (22) into Eq. (20) yields

$$V^N = \frac{\frac{Q_0^N}{Q^N}(1-\xi\theta^C)\left(1 - \frac{Q_0^P}{Q^P}\right)}{[(1-f_A)V_0^N]^{-1} + (f_A A_0 N_i)^{-1}} = D\mu_* \frac{Q^N - Q_0^N}{1 + \zeta Q^N} S_I \tag{A7}$$

which, with Eq. (18), is a cubic equation in Q^N if f_A is known:

$$X = \frac{Q_0^N}{D\mu_* S_I \left\{ [(1-f_A)V_0^N]^{-1} + (f_A A_0 N_i)^{-1} \right\}} \tag{A8}$$

$$Y = \frac{1}{3}\left[\frac{Q_0^P}{r_V} - \zeta(1 - \xi\hat{\theta}^C)X - Q_0^N \right], \quad Z = \frac{Q_0^N Q_0^P}{r_V} + \left[1 - (1 - \zeta Q_0^N)\xi\hat{\theta}^C \right] X \tag{A9}$$

$$Q^N(f_A) = 2\cos\left\{ \frac{1}{3} \operatorname{acos}\left[\sqrt{\frac{6.75}{(3Y^2+Z)^3}} (\xi\hat{\theta}^C Q_0^N X - 2Y^3 - YZ) \right] \right\} \sqrt{Y^2 + \frac{Z}{3}} + \frac{1}{3}\left[Q_0^N + \zeta(1-\xi\hat{\theta}^C)X - \frac{Q_0^P}{r_V} \right] \tag{A10}$$

Eqs. (16) & (A8) to (A10) can then be solved iteratively. Eq. (24) implies the constraints

$$Q^N \le Q^N_{opt} \quad \text{and} \quad Q^P \le Q^P_{max} \tag{A11}$$

Editorial responsibility: Graham Savidge, Portaferry, UK

Submitted: May 27, 2008; Accepted: September 17, 2008
Proofs received from author(s): February 2, 2009